electronics

MDPI

Article

A Review and Comparison of Solid, Multi-Strands and Litz Style PCB Winding

Minh Huy Nguyen and Handy Fortin Blanchette *

Department of Electrical Engineering, École de Technologie Supérieure (ÉTS), 1100 Notre-Dame Street, Montreal, QC H3C 1K3, Canada; huynm2@hcmut.edu.vn

* Correspondence: handy.fortin-blanchette@etsmtl.ca

Received: 30 June 2020; Accepted: 7 August 2020; Published: 16 August 2020

Abstract: At high frequency, AC resistance of a printed circuit board (PCB) winding becomes important and accounts for a large proportion of planar transformer losses. The winding is then influenced by both skin and proximity phenomenon, which makes the current distribution uneven resulting in an increased resistance. The study of improving AC resistance of a PCB winding has been tackled by many researchers. However, the lack of an overview and comparison among improvements has made it difficult to apply those methods to a specific winding. To overcome the above limitations, this paper investigates the pros and cons of three popular AC resistance optimizing methods: optimizing track width of a solid PCB winding, using multi-strands and using Litz style PCB winding. To verify the theoretical analysis, a total of 12 PCBs are simulated by finite element (FEM) and tested in the laboratory. Five criteria are analyzed, including skin resistance, proximity resistance, AC to DC ratio, total AC resistance and complexity are taken into consideration. The results of this study show that optimizing track width method has a significant improvement on AC resistance while the use of Litz PCB is effective for applications that need stable AC resistance in a wide frequency range. The use of parallel strands winding should be carefully considered as there is not significant benefit in both reducing the AC resistance and AC to DC ratio.

Keywords: finite element simulation; Litz style winding; optimize AC resistance; PCB winding comparison; solid PCB winding

1. Introduction

In recent years, the outbreak of the renewable energy industry and electric vehicles have increased the demand for power conversion systems: micro-grid inverter, wireless chargers, bi-directional converters... On the other hand, the development of semiconductor technology with wide band-gap switching components has removed many limitations of power electronics circuits. Electromagnetic devices, which are known to take a lot of space in power converters, become more compact thanks to the increasing of switching frequency to hundreds of kHz [1] and have created potential opportunities for using planar structures with spiral windings to replace conventional transformers. In applications with planar air coils and transformers, PCB winding is widely used because it has excellent repeatability properties compared to Litz or solid copper wires. Moreover, with properly designed dimensions, the leakage inductance and parasitic capacitance will not have much change among products, which have many benefits in ensuring the performance and stability of converters. However, because a large portion of the window area is occupied by insulation, the copper track area is limited resulting in higher current density than conventional transformers. In addition, at high frequency, the skin and proximity effect become serious and winding losses account for a large portion of the total loss of a planar transformer, up to 80% in the transformer with EI64 core at 100 kHz [2].

All above reasons make it important to minimize the AC resistance of PCB winding. Many researches on improving AC resistance of transformer windings have been done previously with key ideas of interleaving windings, arranging positions or adjusting dimensions of each turn to reduce skin and proximity losses. They can be divided into three main research topics as follows.

1.1. Interleaving Windings to Reduce AC Resistance

At high frequency, a conductor is influenced by time-varying magnetic field caused by itself and adjacent conductors, known as skin and proximity effect and increased AC losses. While skin effect losses depend only on the correlation between the size of the conductor and skin depth, proximity effect losses sharply increase with the number of layers and accounts for a majority part of eddy losses inside a windings [3]. The idea of interleaving primary and secondary windings was presented in some previous articles for both conventional and planar transformer and considered as an effective way to reduce the magnetomotive force (MMF) , thus, improving AC losses of windings. In conventional transformers, primary and secondary windings were divided into many layers and wounded alternately around the core. Thanks to alternating layers with opposite currents, the net current in a Ampere contour was decreased in comparison with non-interleaving, thereby reducing MMF and flux density [4] (Figure 1). Some interleaving structures applied in planar transformers were also proposed in References [5–8] including same layer alternating and multi-layers interleaving. In addition, although interleaving methods are well-known for reducing leakage inductance, however, increasing contact area between the primary and secondary windings has increased parasitic capacitance between windings [2,9]. To be specific, fully interleaving planar transformer with four primary and four secondary layers has equivalent primary capacitance 8.1 times higher than non-interleaving transformer [2]. Besides, interleaving structures also made transformers more complicated to manufacture and impossible to design when windings have few turns.

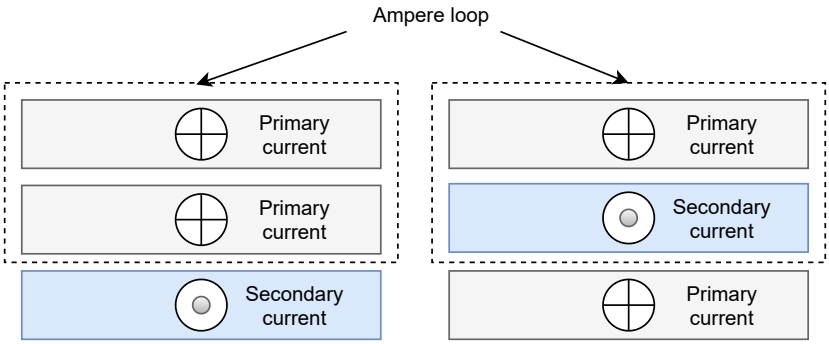

Figure 1. Non-interleaving windings (**Left**) and interleaving windings (**Right**).

1.2. Optimizing AC Resistance by Changing Winding Dimensions

AC resistance was also optimized by adjusting dimensions of a winding to control both skin and proximity effect. For the top-down transformer with foil winding, its dimensions are formatted by a bobbin. Therefore, the foil thickness was adjusted to achieve lowest AC resistance. Simulation and analysis results in References [10,11] showed that the optimum foil thickness depended on the number of layers and tends to decrease with increasing frequency and number of layers. In case of air coil and planar transformers with spiral PCB winding, although the winding's footprint was limited by the size of the magnetic circuit and thickness of copper layers needed to be fitted industrial standard, the track width and track distance could be easily changed by modifying track dimensions and position in circuit design software. Spiral air coil with hollow structure was studied in Reference [12] showed that a maximum quality factor could be achieved by adjusting the ratio between the inner radius and the outer winding radius around 0.45–0.55. In another study by Kim and Park [13], a similar result was also noted when the winding quality factor reached the maximum value as the width of the innermost

loop was a half of the outermost loop. A method to optimize the AC resistance of a winding with the same footprint was proposed in Reference [14]. In this paper, the skin and proximity resistance of a winding can be modified by adjusting its track width and optimized AC resistance occurred when AC to DC ratio of the winding equalled to 4/3 AC to DC ratio caused by skin effect of its conductor.

1.3. Using Multi-Strands and Litz Style PCB Windings to Reduce Skin and Proximity Effect

Litz style PCB winding applied to wireless charging coil and induction cooker were introduced in previous research and considered reducing the AC resistance of a winding. Firstly, a solid track was split to many parallel strands to reduce the skin effect [15,16], thus, reducing the AC to DC ratio of the winding. However, because of the internal proximity effect among strands, the results did not have a significant improvement. A Litz style PCB winding with interleaving strands was proposed in References [17–21]. Because all strands were subjected to the same magnetic field strength, they were expected to carry equal currents and help to reduce AC to DC ratio better than parallel strands winding. However, although these techniques improve AC to DC ratio, both muli-strands and Litz syle PCB need to eliminate a significant portion of the copper area that leads to an increase in DC resistance of the winding. Besides, Litz PCB winding needs to use multiple vias to connect strands on top and bottom layer of the winding. Therefore, it is less reliable than other kinds of PCB windings, especially in cases where the winding operates at high temperature, because the expansion of the insulation layer can destroy the vias.

Although research on improving AC resistance of PCB winding has been done in many previous studies, the lack of a comparison among these methods has caused the limitations of practical applications. Compared to interleaving windings, which is only applicable in a limited number of cases, optimizing the AC resistance by modifying track dimensions and structures are more promising options because they can be applied to many types of winding regardless of the number of turns and layers. To clarify the effectiveness of previous proposed ideas, this paper focuses the analysis and comparison among conductor optimization methods, thereby giving a practical applicability of each case. AC resistance of three popular kinds of windings are studied in a wide range of frequency: solid, multi-strands and Litz style PCB. To have a fair comparison, all windings are assumed to have same dimensions, copper thickness, and track pitch so that they can fit a given footprint.

The rest of paper is organized as follows: winding performance evaluation and analysis are done in Section 2. In Section 3, a number of FEM simulations and measurements are conducted to further describe the AC resistances of different windings. Benefits of each winding type are drawn in Discussion section and a summary is presented in the Conclusions of the paper.

2. Performance Evaluation

2.1. Solid Two Layers Winding Modeling

Considering a cross-sectional area of a two-layer PCB winding, consisting of two stacked conductors (3 and 4) in parallel and two adjacent parallel conductors (1 and 2) as shown in Figure 2. These conductors have the same dimensions, carrying currents in the same direction and as depicted on the figure. At high frequencies, each conductor is affected by both skin and proximity effects of adjacent conductors, causing uneven current distribution across the cross-section and increasing resistance. Each conductor is then subjected to external magnetic field $\overrightarrow{B} = \overrightarrow{B_z} + \overrightarrow{B_x}$ which causes proximity resistances $R_{proximity\_z}$ and $R_{proximity\_x}$, respectively. The per unit AC resistance R_{AC} of a conductor is given by Equation (1) [18]:

$$R_{AC} = R_{skin} + R_{proximity\_z} + R_{proximity\_x} \quad (1)$$

where R_{AC} is the total AC resistance of a conductor, $R_{AC} = R_{DC}$ at 0 kHz. Magnetic fields B_z and B_x can be approximated by using the average value at the center of the conductor's cross-section and they can be assumed to be uniform along the width (W) and thickness (h) of the conductor,

respectively. The excitation currents and B fields are calculated at $I_1 + I_2 = I_3 + I_4 = 1$ A. The total per unit proximity resistance $R_{proximity}$ of conductor 3 is shown in Equation (2) [14,22]:

$$R_{proximity} = R_{proximity\_z} + R_{proximity\_x} = \frac{1}{12} h\omega^2 \sigma B_z^2 \mathrm{W}^3 + \frac{1}{12} \mathrm{W}\omega^2 \sigma B_x^2 h^3 \quad (2)$$

Combining Equations (1) and (2), the per unit length total AC resistance of conductor 3 is drawn:

$$R_{AC} = R_{skin} + R_{proximity\_z} + R_{proximity\_x} = F_{skin} \cdot \frac{1}{\sigma \mathrm{W} h} + \frac{1}{12} h\omega^2 \sigma B_z^2 \mathrm{W}^3 + \frac{1}{12} \mathrm{W}\omega^2 \sigma B_x^2 h^3 \quad (3)$$

where F_{skin} is the AC to DC resistance ratio caused by skin effect and can be calculated by FEM or a 2-D model. In a multi-turns winding where track pitch (P), thickness (t) and copper thickness (h) are constant, Equation (3) is used to calculate AC resistance of a layer of each turn inside the winding. In PCB winding with two layers in parallel, due to symmetry, the current is divided evenly between the two layers and thus, per unit length AC resistance of a two-layer turn calculated as in Equation (4):

$$R_{turn\_2layer} = \frac{1}{2} \left[F_{skin} \cdot \frac{1}{\sigma \mathrm{W} h} + \frac{1}{12} h\omega^2 \sigma B_z^2 W^3 + \frac{1}{12} W\omega^2 \sigma B_x^2 h^3 \right] \quad (4)$$

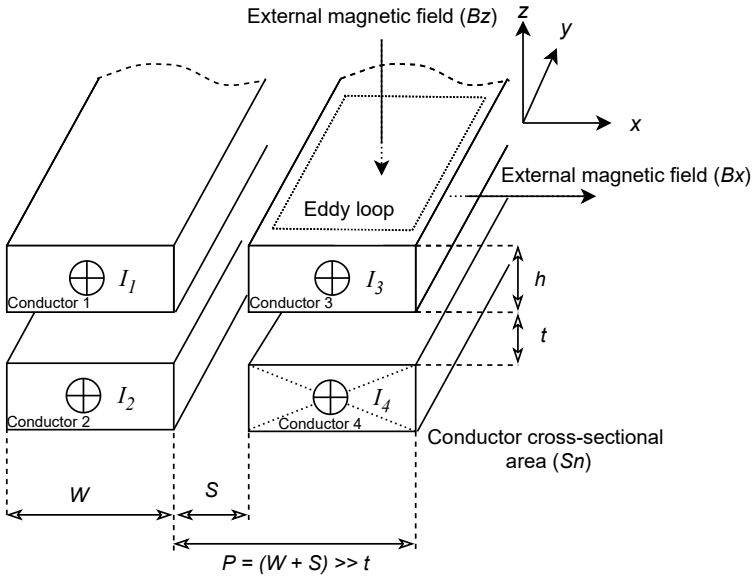

Figure 2. A copper track under external field.

2.2. Two-Layer Multi-Strands Winding

The idea of multi-strands PCB conductor is shown in Figure 3. A solid conductor with conductivity σ and width (W) is cut into many small parallel conductors with same dimensions and gap, the total width of strands and gaps is equal to the width of a solid conductor. By doing that, the eddy loop is reduced and thereby, reducing the AC resistance of the conductor. A multi-strand conductor can be treated as modified solid conductor with virtual conductivity $\sigma' = \eta\sigma$, where η is porosity factor and calculated as in reference [23]. Per unit length AC resistance of one turn of a two-layer winding is then calculated by replacing σ' in Equation (4) as in Equation (5):

$$R_{AC} = F_{skin\_multi-strands} \cdot \frac{1}{2\sigma N d h} + \frac{1}{24} h\omega^2 \sigma B_z^2 \left(\sqrt[3]{\frac{Nd}{W}} W \right)^3 + \frac{1}{24} (Nd) \omega^2 \sigma B_x^2 h^3 \quad (5)$$

where N is the number of strands of each layer of multi-trands winding. Although this structure is expected to reduce AC resistance, the multi-strands conductor still has limitations since outer strands have higher net current than inner strands due to higher electric field. To overcome this problem, Litz style PCB winding with interleaving strands was introduced.

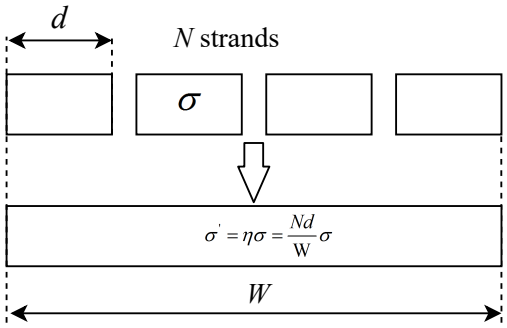

Figure 3. Equivalent model of multi-strands conductor.

2.3. Litz Style PCB Winding

Litz style PCB with interleaving strands was first applied to planar structures and they are expected to have better AC resistance in comparison to solid PCB winding. Firstly, a one-layer solid conductor is cut into N strands. After that, the strands' positions are gradually changed from the bottom to top layer and from the topmost to the bottommost side thanks to the use of two-layer PCB and vias as in Figure 4. By doing that, Litz style PCB has haft number of strands compared to two-layer multi-strands PCB with the same footprint and each strand is subjected to the same magnetic field, resulting in uniform current density among all strands. Moreover, because the distance between strands is large in comparison with strand width, Litz style PCB is supposed to have a significant reduction of both internal and external proximity resistances. The per unit length AC resistance of winding is just skin resistance and is expressed as in Equation (6):

$$R_{AC} = R_{skin} = F_{skin\_Litz} \cdot \frac{1}{\sigma N d h} \tag{6}$$

where N is also defined as the number of strands of Litz winding (N = 5 with the design in Figure 4), d and W are the strand width and track width, respectively.

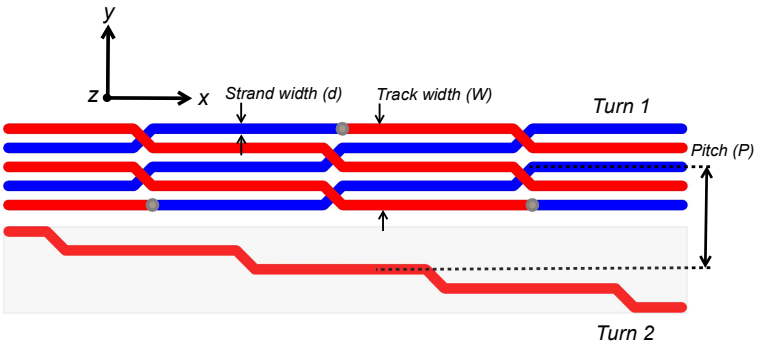

Figure 4. Two-layer Litz style PCB tracks with top layer in red, bottom layer in blue (**Upper track**) and an extracted interleaving strand (**Lower track**).

2.4. Performance Comparison

To have an effective comparison, the windings are designed with the same footprint and dimension. Firstly, the solid winding is designed with maximum allowable track width, $W = W_{\max}$. After that, the multi-strands two-layer winding with the same footprint is done by stretching $2N$ small parallel strands to fit the track width W_{max}, each strand has width d and total copper width in each layer is $W_{Cu-MultiStrands} = Nd < W_{max}$. Finally, the Litz style winding is created by interleaving N strands on two layers. A total of four different designs are considered as in Table 1. Some assumptions need to be included in the calculation:

- The track pitch (P) is many times larger than PCB thickness (h) and the redistribution of current density in each track at high frequency does not affect on its external fields.
- The Litz style winding is considered to completely remove proximity resistance.
- The skin ratio (F_{skin}) is considered to have a slight change while changing the track width [14].

Table 1. Two layers PCB profiles and parameters.

No	Profile Names	Track Width	Track Pitch	Strand Width	Total Number of Strands N_{total}
PCB1	Solid with maximum track width	$W_{\max}$	P	-	-
PCB2	Solid with reduced track width	Nd	P	-	-
PCB3	Multi-strands	$W_{\max}$	P	d	$2N$
PCB4	Litz style PCB	$W_{\max}$	P	d	N

DC resistances, AC resistances, including skin, and proximity resistances are taking into account for comparison. The per unit length resistances of each turn of a winding is summarized as in Table 2.

Table 2. Per unit length resistances of each turn of different windings.

No	Profile Names	DC Resistance	Skin Resistance	Proximity Resistance
PCB1	Solid with maximum track width	$\frac{1}{2\sigma W_{\max} h}$	$\frac{F_{skin\_solid}}{2\sigma W_{\max} h}$	$\frac{1}{24} h\omega^2\sigma B_z^2 W_{\max}^3 + \frac{1}{24} W_{\max}\omega^2\sigma B_x^2 h^3$
PCB2	Solid with reduced track width	$\frac{1}{2\sigma Ndh}$	$\frac{F_{skin\_solid}}{2\sigma Ndh}$	$\frac{1}{24} h\omega^2\sigma B_z^2 (Nd)^3 + \frac{1}{24} (Nd)\,\omega^2\sigma B_x^2 h^3$
PCB3	Multi-strands	$\frac{1}{2\sigma Ndh}$	$\frac{F_{skin\_multi-strands}}{2\sigma Ndh}$	$\frac{1}{24} h\omega^2\sigma B_z^2 (Nd) W_{\max}^2 + \frac{1}{24} (Nd)\,\omega^2\sigma B_x^2 h^3$
PCB4	Litz style PCB	$\frac{1}{\sigma Ndh}$	$\frac{F_{skin\_Litz}}{\sigma Ndh}$	≈ 0

Table 2 shows the variation of AC resistances when applying various improvement methods. The change in conductor width does not have much improvement on skin ratios, i.e., at frequency 700 kHz, skin ratio has changed from 1.5 to 1.3 when reducing track width of 2 oz copper track from 5 mm to 2 mm, respectively [14]. Therefore, the skin resistance is considered to proportion to the copper area and $R_{skin-PCB1} < R_{skin-PCB2} \approx R_{skin-PCB3} < R_{skin-PCB4}$. Proximity resistance of PCB 1 is the highest in the group because it has the larger copper width. PCB 2 has an improvement in proximity resistance in comparison to PCB 3 because it has a smaller $R_{proximity\_z}$ than PCB 3. The initial analysis shows that cutting a solid winding into strands is not better than reducing track width. Finally, in the idea Litz style PCB, the proximity effects are completely removed and it has very good AC to DC ratio, but in return, removing too much copper has significantly increased skin resistance, that can make total resistance worse than solid and multi-strands windings with same track width and number of layers.

3. Simulation and Measurement Results

In power converter with rated power to a few KVA, the switching frequency range from several kHz to 1 MHz and PCB windings with 1 oz and 2 oz copper weight are mostly used. In total, 12 windings are designed to verify the analysis results with one, three and seven turns and divided

into three groups with the same number of turns and footprints. Firstly, the maximum track width of all groups is set at $W_{max} = 5$ mm and track pitch is kept constant at $P = 6$ mm. After that, various improvement methods are applied to these windings to reduce AC resistance. It includes reducing track width, cutting into multiple strands and using Litz structure. The number of strands and strand width are chosen $N_{total} = 10$, $d = 0.6$ mm for multi-strands and $N_{total} = 5$, $d = 0.6$ mm for Litz windings based on the design in Reference [24], which was known to have a very good improvement on AC to DC ratio. The parameters in detail are shown in Table 3 and sample designs are presented in Figure 5.

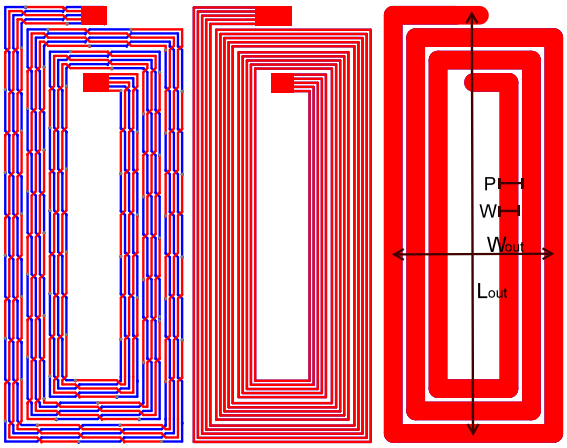

Figure 5. Litz PCB 3 turn winding (**Left**), multi-strands winding (**Middle**) and solid PCB winding (**Right**).

Simulations are done by Ansys Maxwell with 3-D models and AC resistances are simulated at the following frequencies: 5 kHz (equivalent to DC), 200 kHz, 300 kHz, 500 kHz and 700 kHz. PCB parameters are chosen with copper thickness of 0.07 mm and insulator thickness of 1.62 mm, copper conductivity is set $\sigma = 52.5 \times 10^6$ S/m and insulator relative permeability 1.65. AC resistances which have been extracted from PCBs 1–8 simulations indicate the total AC resistances of windings with different designs. Because simulated AC resistances cannot be separated by skin and proximity resistance, a number of simulations and measurements need to be done with one turn one layer winding as in PCBs 9–12. AC resistances of these windings are known as skin resistance and AC to DC ratios, which are ratios between AC and DC resistance of each design at a specific frequency, are used to calculated skin resistance of windings with many turns. Following that, proximity resistances are calculated by the difference between total AC resistance and skin resistance as in Equation (7). Where F_{skin} is the ratio of AC to DC resistance of one turn one layer winding, R_{AC} is the total AC resistance of a winding at a given frequency.

$$R_{skin} = F_{skin} \cdot R_{DC} \tag{7}$$

$$R_{proximity} = R_{AC} - R_{skin} \tag{8}$$

Table 3. Two ounces two-layer winding parameters.

Group	No	Descriptions	Number of Turns	Outer Length L_{out} (mm)	Outer Width W_{out} (mm)	Track Width W (mm)	Strand Width d (mm)	Total Number of Strands N_{total}
Group 1	PCB 1	Solid winding 2 layers	3	112	43	5	-	-
	PCB 2	Solid winding 2 layers	3	112	43	3	-	-
	PCB 3	Multi-strands winding 2 layers	3	112	43	5	0.6	10
	PCB 4	Litz winding 2 layers	3	112	43	5	0.6	5
Group 2	PCB 5	Solid winding 2 layers	7	160	91	5	-	-
	PCB 6	Solid winding 2 layers	7	160	91	3	-	-
	PCB 7	Multi-strands winding 2 layers	7	160	91	5	0.6	10
	PCB 8	Litz winding 2 layers	7	160	91	5	0.6	5
Group 3	PCB 9	Solid winding 1 layer	1	160	91	5	-	-
	PCB 10	Solid winding 1 layer	1	160	91	3	-	-
	PCB 11	Multi-strands winding 1 layer	1	160	91	5	0.6	5
	PCB 12	Litz winding 2 layers	1	160	91	5	0.6	5

All windings are then produced with the same dimensions and specifications with simulated PCBs. Vector Analyzer Agilent E5061B is employed and ports 1–2 shunt method is used for resistance measurements. The designed fixture with two SMA–SMA connectors is made up as in Figure 6 and connected to PCB under test by six parallel Litz wires. By doing that, the AC resistance of the fixture is kept low in the frequency range to 700 kHz so it does not affect the measurement results. DC resistances of all windings are presented in Table 4. Simulation and experimental AC resistances of three case studies are plotted in the same graph to assess suitability as well as to verify the approximation analysis used.

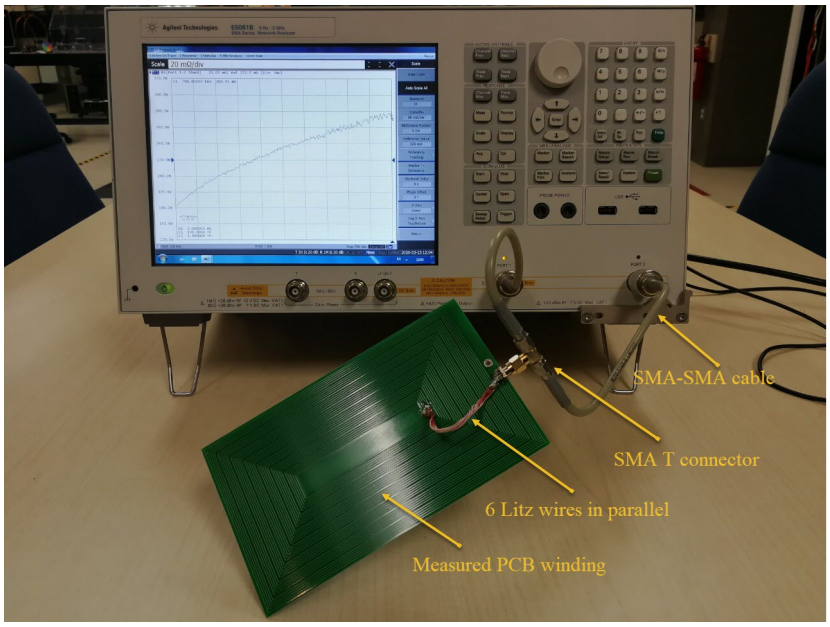

Figure 6. Measurement setup.

Table 4. DC resistances of PCB prototypes.

Group	PCBs	Descriptions	$R_{DC-measure}$ mΩ	$R_{DC-simulate}$ mΩ	$\lvert R_{DC-measure} - R_{DC-simulate} \rvert$ mΩ
Group 1 (Three-Turn PCBs)	PCB 1	solid 5 mm	22.5	21.28	0.7
	PCB 2	solid 3 mm	33.1	34.78	1.68
	PCB 3	multi-strands	38.2	35.27	2.93
	PCB 4	Litz PCB	74	70.57	3.43
Group 2 (Seven-Turn PCBs)	PCB 5	solid 5 mm	65.3	69.83	4.53
	PCB 6	solid 3 mm	107.1	114	6.9
	PCB 7	multi-strands	107.96	114.5	6.54
	PCB 8	Litz PCB	222	226.64	4.64
Group 3 (One-Turn PCBs)	PCB 9	solid 5 mm	24.57	26.5	1.93
	PCB 10	solid 3 mm	43.2	44.1	0.9
	PCB 11	multi-strands	39.76	43.54	3.78
	PCB 12	Litz PCB	38.61	44.89	6.28

3.1. Case Study 1: 1-Turn 1-Layer PCB Windings

In the first study, the PCB windings are designed with the same dimension but different styles as in Figure 7. By removing the second layer and reducing the number of turns to only one, it allows to observe the skin effect only. In the case of Litz style PCB, it is necessary to use two layers to interleave strands together, so it is impossible to design one layer PCB like one did for solid or multi-strands winding. However, because the Litz PCB is known removing a large part of its proximity resistance, in 1 turn design, it can be considered to be affected by skin resistance only. Hence, PCBs 10, 11, 12 have the same cross-sectional area and same initial DC resistance while PCB 9 has lowest DC

resistance because of its largest copper width. Simulated and measured AC resistances are shown in Figure 8 (Left) and skin ratios are calculated in Figure 8 (Right).

Because Litz winding has two copper layers but solid and multi-strands winding have one layer only. Therefore, to ensure a fair comparison, skin resistance of Litz PCB (PCB 12) is compared to the equivalent skin resistance of a two-layer winding with the same footprint which is a half value of AC resistance of PCBs 9, 10 and 11 and shown in Figure 9. The results show that despite the improvement in the skin ratio, the need to remove too much copper area made the skin resistance of Litz style winding much higher than the other windings. At 500 kHz, F_{skin} of Litz style PCB is equal to 76% of solid 5 mm. However, the cross-sectional area is just 30% in comparison with solid 5 mm two layers. A similar result is also obtained when comparing Litz PCB with multi-strands and solid 3 mm. For solid and multi-strands winding with the same cross-sectional area, as in PCB 10 and 11, the improvement in skin ratio and skin resistance is negligible, the difference is about 5–8% at 500 kHz and 700 kHz. These simulations and measurements are in accordance with theoretical analysis in the previous section. Furthermore, F_{skin} values will be used to separate skin and proximity resistances in studies 2 and 3.

Figure 7. Single turn PCB windings with solid 5 mm (**Top Left**), solid 3 mm (**Top Right**), multi-strands (**Bottom Left**) and Litz style (**Bottom Right**).

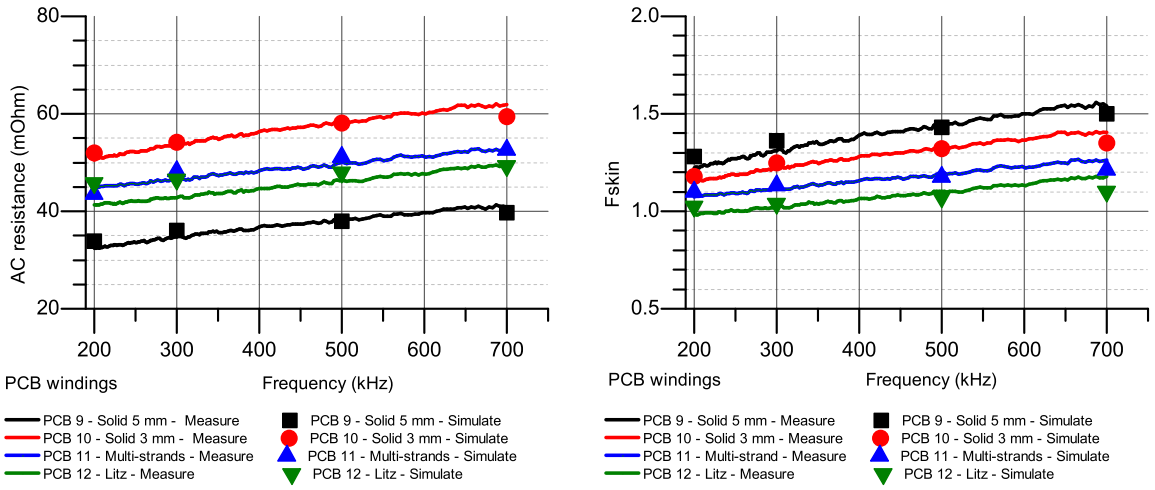

Figure 8. Simulated and measured skin resistances (**Left**) and skin ratio (**Right**) of different windings.

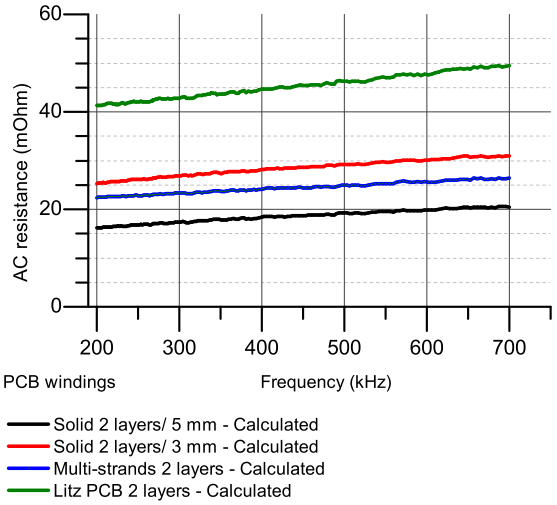

Figure 9. Calculated equivalent skin resistances of one turn two layers windings.

3.2. Case Study 2: 3-Turn 2-Layer PCB Windings

In this study, all two-layer windings have three turns with dimensions as in PCBs 1, 2 and 3 in Table 3 and Figure 10. Skin and proximity resistances are calculated based on skin ratio in Case Study 1 and Equation (7). AC resistances, including simulated and measured resistances in Figure 11 show the appropriateness of simulation and experimental results. The results show that in a winding with few turns, it is not necessary to apply improving method since solid winding already has good AC resistance. This can be explained by considering the contribution of skin and proximity resistance on the total AC resistance of a winding in Figures 12–14. At 500 kHz, these values are $R_{skin\_5\,mm} = 32.5\,\text{m}\Omega$ and $R_{proximity\_5\,mm} = 34\,\text{m}\Omega$, the contribution of proximity resistance is equal to skin resistance. Therefore, reducing the proximity resistance by reducing track width or using multi-strands winding has no significant improvement, since it has increased the skin resistance. In comparison between multi-strands and solid PCB with the same cross-sectional area, the proximity resistance of multi-strands winding (PCB3) is larger than solid (PCB2) at 500 kHz and 700 kHz. This measurement result is consistent with the previous conclusion that there is no improvement with proximity resistance when cutting solid winding into small strands in parallel. Finally, the Litz style winding has the best AC to DC ratio with proximity resistance almost eliminated. However, because of the smallest cross-sectional area, it has the largest AC resistance among the windings.

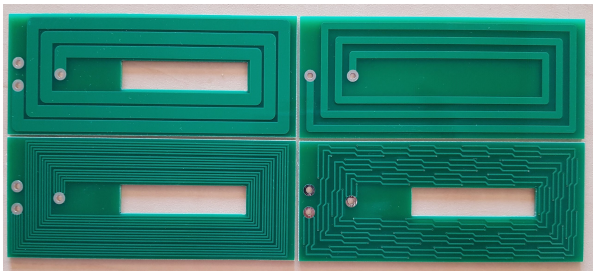

Figure 10. Three turn PCB windings with solid 5 mm (**Top left**), solid 3 mm (**Top right**), multi-strands (**bottom left**) and Litz style (**bottom right**).

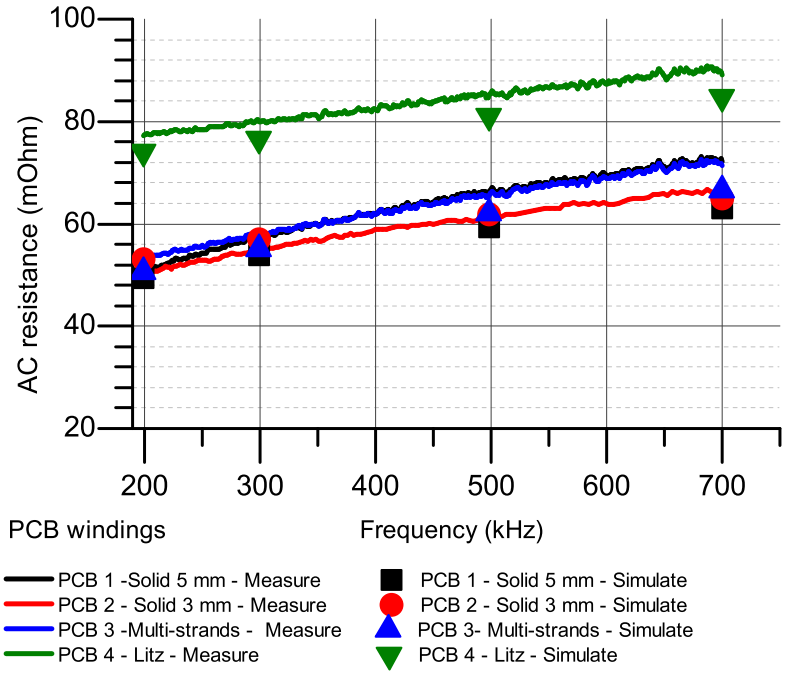

Figure 11. Measured and simulated AC resistances of 3-turn windings.

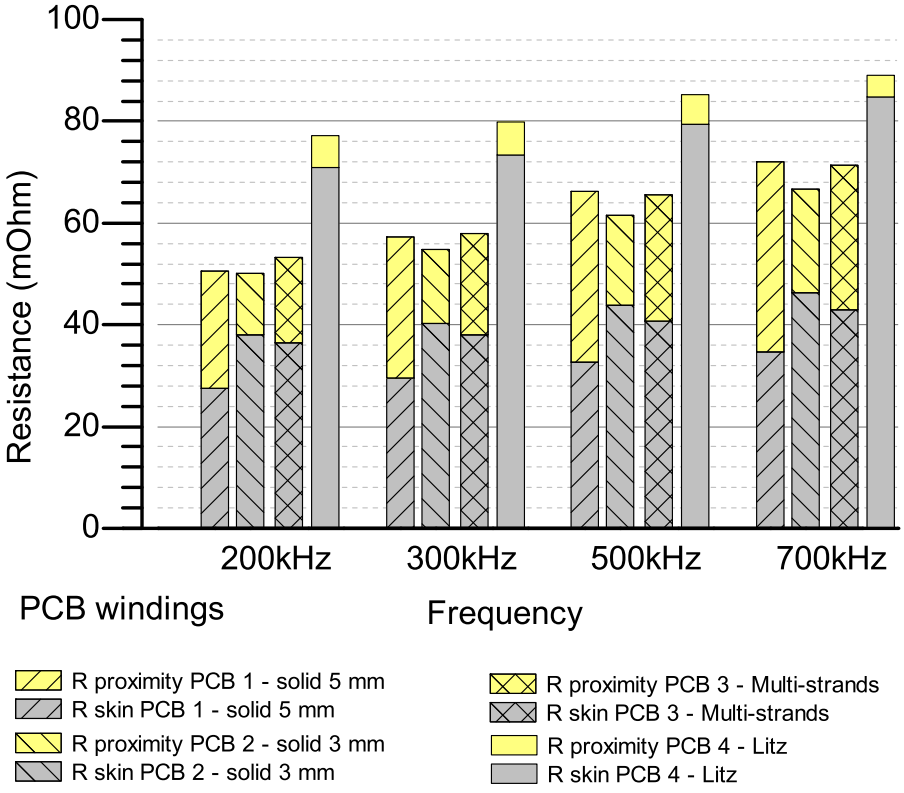

Figure 12. Calculated skin and proximity resistances of 3-turn windings.

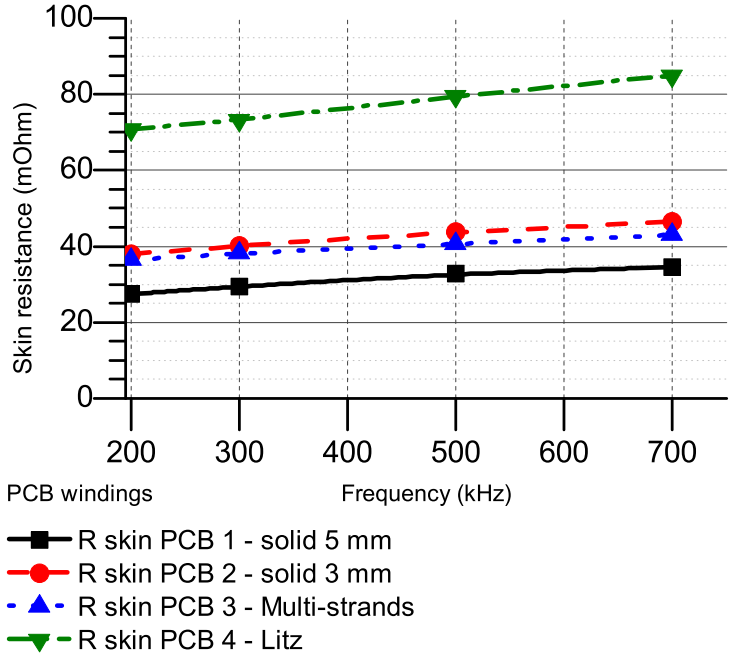

Figure 13. Calculated skin resistances of 3-turn windings.

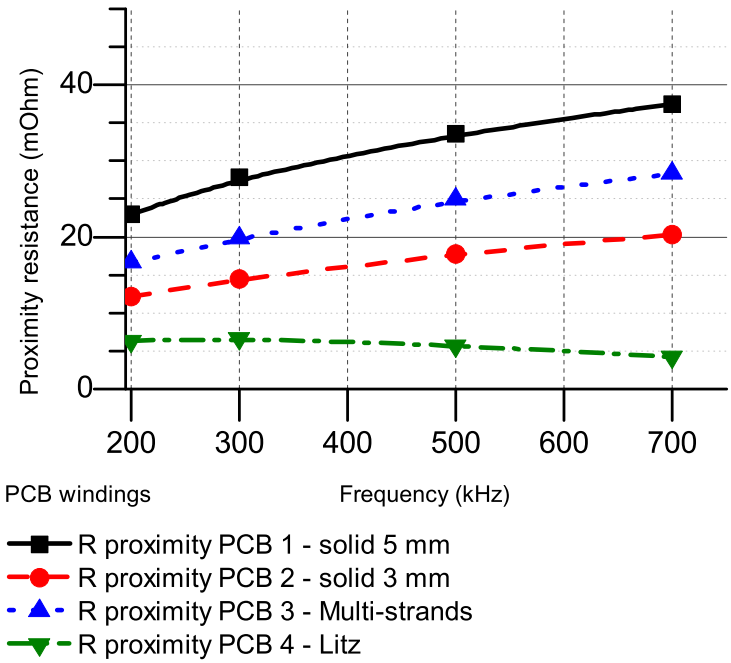

Figure 14. Calculated proximity resistances of 3-turn windings.

3.3. Case Study 3: 7-Turn 2-Layer PCB Windings

In the last study, windings are designed with seven turns as in PCB 5, 6, 7, 8 on Table 3 and Figure 15. The measurement and simulation steps are also repeated as in Case Study 2 and results are shown in Figures 16–19. PCB 5 with track width 5 mm has the highest AC resistance because it is mostly influenced by proximity effect. At 500 kHz, these values are $R_{skin\_PCB5} = 95\,\text{m}\Omega$ and $R_{proximity\_PCB5} = 215\,\text{m}\Omega$, which proximity resistance is about 2.26 times compared to skin resistance. Therefore, optimal methods need to be applied to reduce this value. Optimal methods show a significant improvement in AC resistance at high frequency because they have eliminated a majority

of proximity resistance. These values are $R_{proximity\_PCB6} = 85\,\text{m}\Omega$, $R_{proximity\_PCB7} = 103\,\text{m}\Omega$ and $R_{proximity\_PCB8} = 10\,\text{m}\Omega$ at 500 kHz, which is many times smaller than proximity resistance of PCB 5. PCB 5 and 6 have the same AC resistance in the frequency range to 500 kHz and then the AC resistance of PCB 5 is smaller than PCB 6 at 700 kHz. This is consistent with the theoretical analysis in the previous section and again shows the stranded winding does not have much help in reducing AC resistance compared to reducing track width. Litz PCB in applications with many turns windings has shown a significant improvement in AC resistance compared to maximum track width. However, because of keeping AC resistance stable at high value in a wide frequency range has made worse losses in the low frequency region.

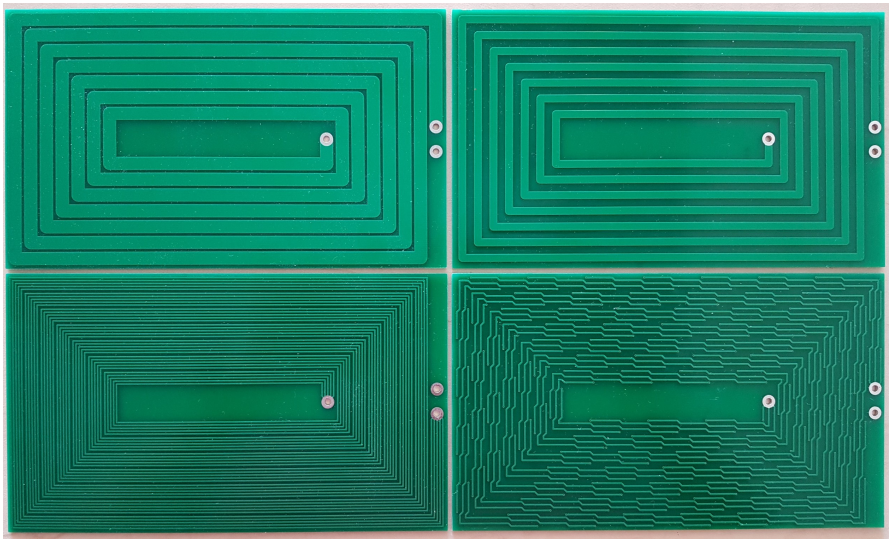

Figure 15. Seven-turn PCB windings with solid 5 mm (**Top left**), solid 3 mm (**Top right**), multi-strands (**bottom left**) and Litz style (**bottom right**).

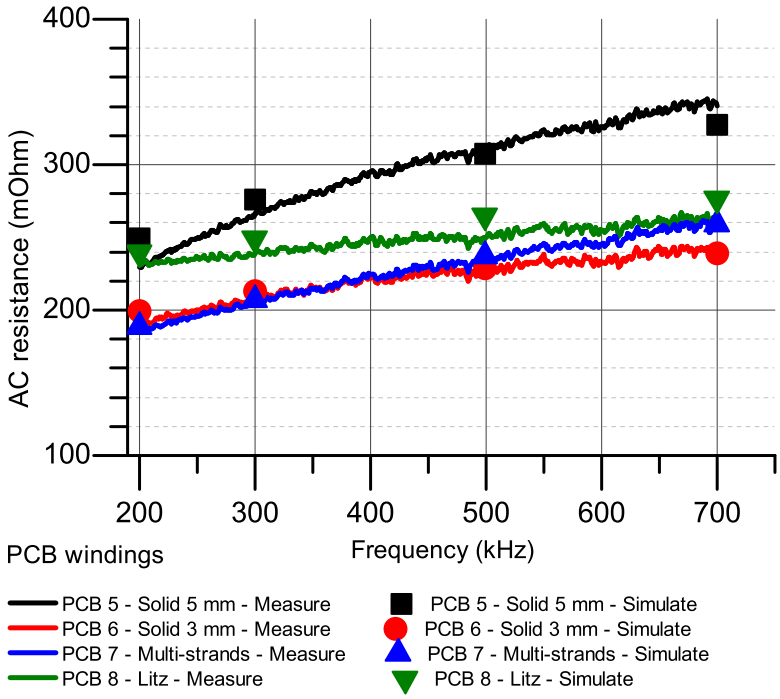

Figure 16. Measured and simulated AC resistances of 7-turn windings.

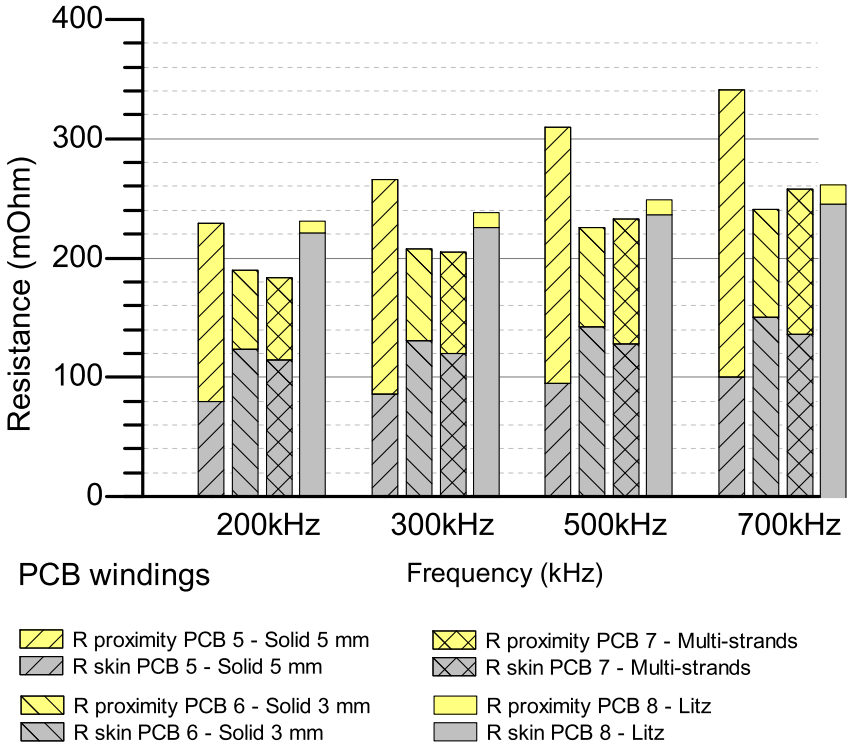

Figure 17. Calculated skin and proximity resistances 7-turn windings.

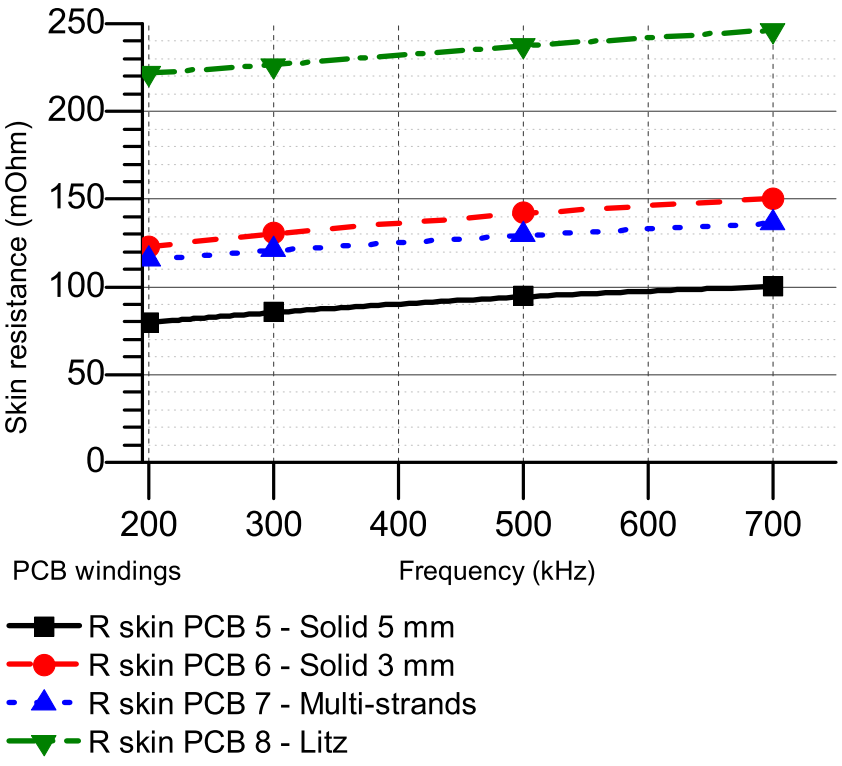

Figure 18. Calculated skin resistances of 7-turn windings.

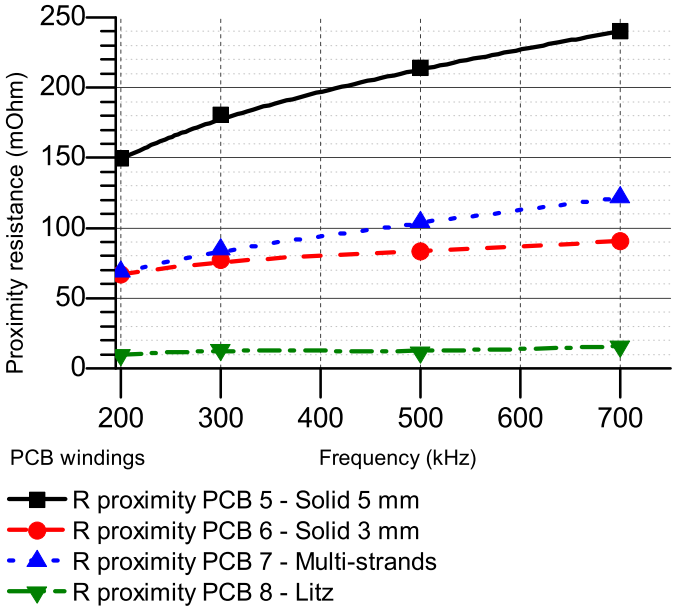

Figure 19. Calculated proximity resistances of 7-turn windings.

4. Discussion

4.1. AC Resistances at Higher Frequency

To better understand the behaviour of different PCB windings, measurements are done in a range from 1 MHz to 15 MHz, which is known as frequency range of higher order harmonics of power converters. Because impedance of 3-turn and 7-turn PCB windings become larger in this range, the port 2 reflection method is used to measure and extract AC resistances and impedance of PCBs 1–8 windings. Measurement results in Figure 20 show that improving AC resistance by reducing track width still gives a good result over a wide range of frequency.

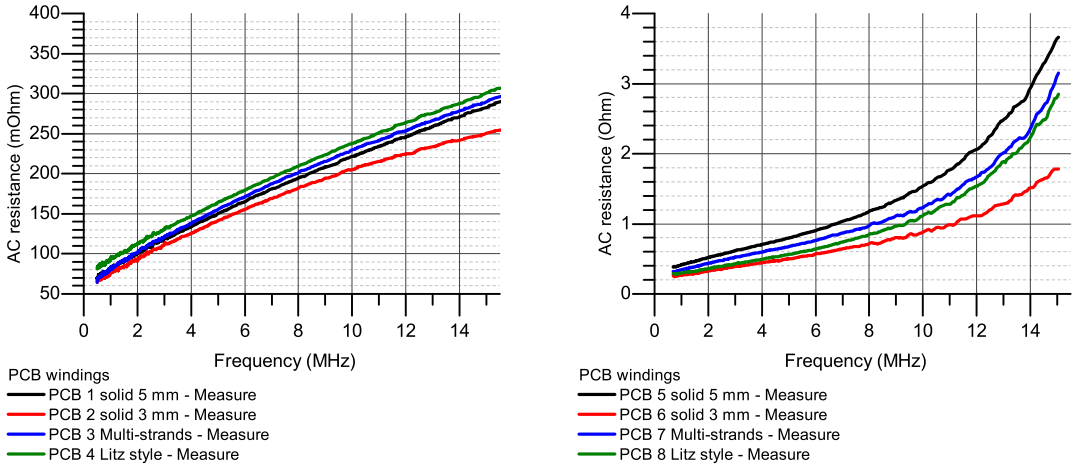

Figure 20. AC resistances of 3-turn windings (**Left**) and 7-turn windings (**Right**) at higher frequency range.

4.2. Pros and Cons of Each Winding Style

Simulation and measurement results, along with mathematical analysis, have shown the pros and cons of each improvement. The AC to DC ratios between the two winding groups with different number of turns in Figure 21 show that Litz PCB has a stable total AC resistance to DC resistance ratio (F_r) when both the frequency and number of turns of windings have changed. However, the need to

eliminate a large copper area has made Litz winding worse resistance than adaptive solid winding. Figure 21 also shows that the Fr value should not be used to evaluate the improvement of AC resistance and the performance of an optimal method. Therefore, five comparison points, including skin resistance, proximity resistance, AC to DC ratio, total AC resistance and complexity should be taken into consideration when choosing a PCB winding design, as presented in Figure 22. At low frequency, the winding resistance is determined by skin resistance, which is directly related and tends to decrease as the conductance cross-sectional area increases. At high frequency, or when the proximity effect becomes serious, optimal methods should be applied to reduce winding losses. The use of multi-strand winding is not recommended due to its complex design and unclear performance while the use of solid PCB with optimal track width shows a clearer improvement in AC resistance. Litz style PCB, which is well known for its AC on DC ratios and very good proximity resistance should be used for winding that have many turns or in equipment that needs stability of resistance in a wide frequency range.

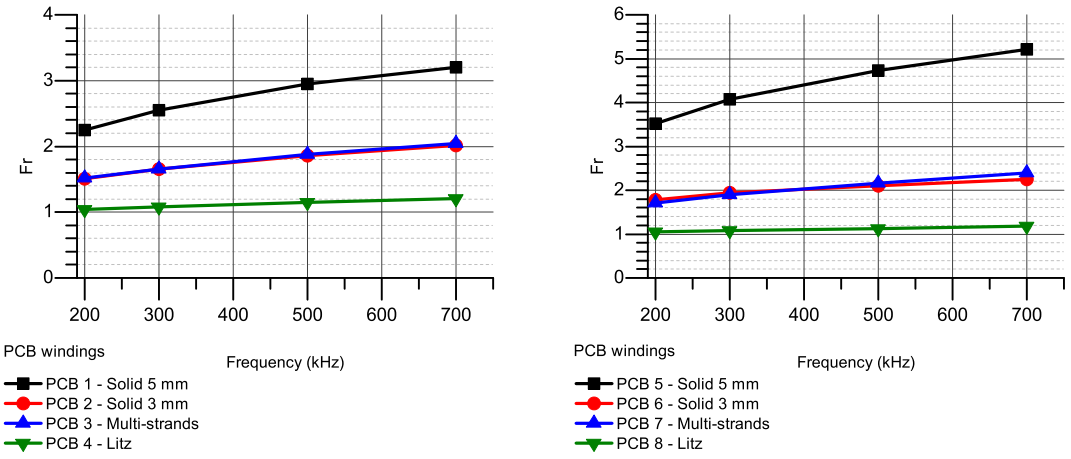

Figure 21. Calculated AC to DC ratio of 3-turn windings (**Left**) and 7-turn windings (**Right**).

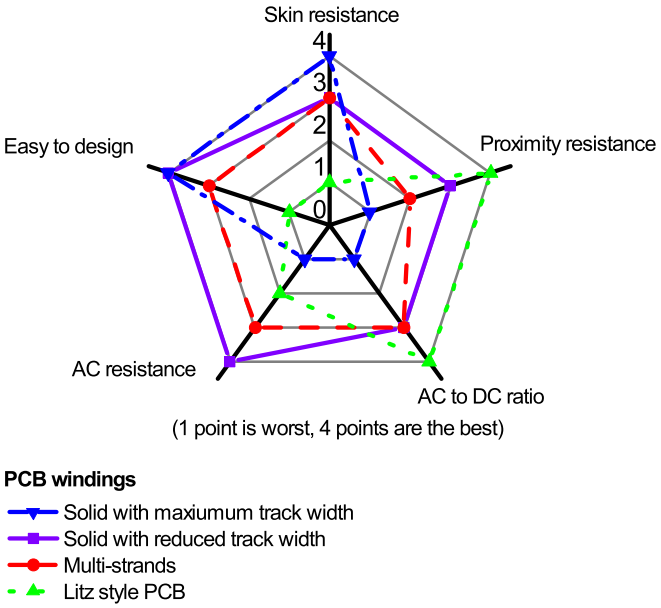

Figure 22. Comparison among PCB winding design methods with high impact of proximity effect.

5. Conclusions

This paper has presented a general review of improving methods applied to the reduction of AC resistance of a PCB winding and shows the advantages and disadvantages of each improvement. It also points out the need to use absolute AC resistance as a main comparing factor in designs PCB winding, instead of AC to DC ratio. In addition, this paper also shows the contribution of skin and proximity resistance in a winding and with a conclusion that: at high frequency, the AC resistance of a winding is greatly affected by proximity resistance while at low frequency, skin resistance is decisive for the AC resistance of a winding. Thus, an appropriate method should be used for each application.

Author Contributions: M.H.N. did the analysis, simulations and verified the results with measurement prototypes. H.F.B. provided supervision and manuscript revised. All authors have read and agreed to the published version of the manuscript.

Funding: This research has been funded by the NSERC under grant number RGPIN 2019-07128.

Conflicts of Interest: The authors declare no conflict of interest.

Abbreviations

The following abbreviations are used in this manuscript:

σ	Copper conductivity
δ	Copper skin depth
ω	Angular frequency
B_x	Average external magnetic field parallel to X Axis
B_z	Average external magnetic field parallel to Z Axis
d	Strand width
FEM	Finite element simulation
F_{skin}	Ratio of AC resistance causes by skin effect to DC resistance
$F_{proximity}$	Ratio of AC resistance causes by proximity effect to DC resistance
F_r	Ratio of total AC resistance to DC resistance
h	Track thickness
I	Excitation current or main current
L_{out}	Outer length of a winding
MMF	Magnetomotive Force
N	Number of strands of one layer of multi-strand winding or Number of strands of Litz style winding
N_{total}	Total number of strands of a winding
P	Track pitch
R_{AC}	Total AC resistance causes by skin and proximity effects
R_{DC}	DC resistance
R_{skin}	AC resistance causes by skin effect
$R_{proximity}$	AC resistance causes by proximity effect
S	Track distance
t	PCB thickness or layer distance
VNA	Vector Network Analyzer
W	Track width
W_{out}	Outer width of a winding

References

1. Li, B.; Li, Q.; Lee, F.C. High-Frequency PCB Winding Transformer With Integrated Inductors for a Bi-Directional Resonant Converter. *IEEE Trans. Ind. Electron.* **2019**, *34*, 6123–6135. [CrossRef]
2. Ouyang, Z.; Thomsen, O.C.; Andersen, M.A.E. Optimal Design and Tradeoff Analysis of Planar Transformer in High-Power DC–DC Converters. *IEEE Trans. Ind. Electron.* **2012**, *59*, 2800–2810. [CrossRef]
3. Marian K. Kazimierczuk, Proximity Effect. In *High Frequency Magnetic Components*, 2nd ed.; Wiley: Coshocton, OH, USA, 2014; p. 226.

4. Barrios, E.L.; Urtasun, A.; Ursúa, A.; Marroyo, L.; Sanchis, P. High-Frequency Power Transformers with Foil Windings: Maximum Interleaving and Optimal Design. *IEEE Trans. Ind. Electron.* **2015**, *30*, 5712–5723. [CrossRef]
5. Zhao, B.; Ouyang, Z.; Anderson, M.A.E.; Duffy, M.; Hurley, W.G. An improved partially interleaved transformer structure for high-voltage high-frequency multiple-output applications. In Proceedings of the IECON 2017-43rd Annual Conference of the IEEE Industrial Electronics Society, Beijing, China, 29 October–1 November 2017; pp. 798–804.
6. Youssouf, K.; Kahlouche, F.; Soultan, M.; Youssouf, M.; Bechir, M.H.; Capraro, S.; Chatelon, J.P.; Siblini, A.; Siblini, J.J. Design and Study of Interleaved and Face to Face Magnetic Microtransformers. *IEEE Trans. Electron. Devices* **2014**, *61*, 2873–2878. [CrossRef]
7. Thummala, P.; Schneider, H.; Zhang, Z.; Andersen, M.A.E. Investigation of Transformer Winding Architectures for High-Voltage (2.5 kV) Capacitor Charging and Discharging Applications. *IEEE Trans. Ind. Electron.* **2016**, *31*, 5786–5796. [CrossRef]
8. Lee, C.K.; Su, Y.P.; Hui, S.Y.R. Printed Spiral Winding Inductor With Wide Frequency Bandwidth. *IEEE Trans. Ind. Electron.* **2011**, *26*, 2936–2945. [CrossRef]
9. Saket, M.A.; Shafiei, N.; Ordonez, M. Planar transformer winding technique for reduced capacitance in LLC power converters. In Proceedings of the 2016 IEEE Energy Conversion Congress and Exposition (ECCE), Milwaukee, WI, USA, 18–22 September 2016; pp. 1–6. [CrossRef]
10. Stadler, A.; Albach, M.; Macary, F. The minimization of copper losses in core-less inductors: Application to foil- and PCB-based planar windings. In Proceedings of the 2005 European Conference on Power Electronics and Applications, Dresden, Germany, 11–14 September 2005. [CrossRef]
11. Marian, K. Kazimierczuk, Winding resistance at high frequencies. In *High Frequency Magnetic Components*, 2nd ed.; Wiley: Coshocton, OH, USA, 2014; p. 303.
12. Su, Y.; Liu, X.; Lee, C.K.; Hui, S.Y. On the relationship of quality factor and hollow winding structure of coreless printed spiral winding (CPSW) inductor. *IEEE Trans. Ind. Electron.* **2012**, *27*, 3050–3056.
13. Kim, D.-H.; Park, Y.-J. Calculation of the inductance and AC resistance of planar rectangular coils. *Electron. Lett.* **2016**, *52*, 1321–1323. [CrossRef]
14. Nguyen, M.H.; Fortin Blanchette, H. Optimizing AC Resistance of Solid PCB Winding. *Electronics* **2020**, *9*, 875. [CrossRef]
15. Varghese, B.J.; Smith, T.; Azad, A.; Pantic, Z. Design and optimization of decoupled concentric and coplanar coils for WPT systems. In Proceedings of the 2017 IEEE Wireless Power Transfer Conference (WPTC), Taipei, Taiwan, 10–12 May 2017; pp. 1–4.
16. Lope, I.; Carretero, C.; Acero, J.; Burdío, J.M.; Alonso, R. PCB multi-track coils for domestic induction heating applications. In Proceedings of the IECON 2012-38th Annual Conference on IEEE Industrial Electronics Society, Montreal, QC, Canada, 25–28 October 2012; pp. 3287–3292.
17. Serrano, J.; Lope, I.; Acero, J.; Carretero, C.; Burdío, J.M. Mathematical description of PCB-adapted litz wire geometry for automated layout generation of WPT coils. In Proceedings of the IECON 2017-43rd Annual Conference of the IEEE Industrial Electronics Society, Beijing, China, 29 October–1 November 2017; pp. 6955–6960.
18. Lope, I.; Carretero, C.; Acero, J.; Alonso, R.; Burdío, J.M. AC Power Losses Model for Planar Windings with Rectangular Cross-Sectional Conductors. *IEEE Trans. Ind. Electron.* **2014**, *29*, 23–28. [CrossRef]
19. Wang, S.; de Rooij, M.A.; Odendaal, W.G.; van Wyk, J.D.; Boroyevich, D. Reduction of high-frequency conduction losses using a planar litz structure. *IEEE Trans. Ind. Electron.* **2005**, *20*, 261–267. [CrossRef]
20. Lope, I.; Acero, J.; Serrano, J.; Carretero, C.; Alonso, R.; Burdio, J.M. Minimization of vias in PCB implementations of planar coils with litz-wire structure. In Proceedings of the 2015 IEEE Applied Power Electronics Conference and Exposition (APEC), Charlotte, NC, USA, 15–19 March 2015; pp. 2512–2517.
21. Rehlaender, P.; Grote, T.; Tikhonov, S.; Niejende, H.; Schafmeister, F.; Bocker, J.; Thiemann, P. A PCB Integrated Winding Using a Litz Structure for a Wireless Charging Coil. In Proceedings of the 2019 21st European Conference on Power Electronics and Applications (EPE'19 ECCE Europe), Genova, Italy, 2–5 September 2019; pp. P.1–P.9.
22. Kuhn, W.B.; Ibrahim, N.M. Analysis of current crowding effects in multiturn spiral inductors. *IEEE Trans. Microw. Theory Tech.* **2001**, *49*, 31–38. [CrossRef]

23. Hurley, W.G.; Gath, E.; Breslin, J.G. Optimizing the AC resistance of multilayer transformer windings with arbitrary current waveforms. *IEEE Trans. Ind. Electron.* **2000**, *15*, 369–376. [CrossRef]
24. Lope, I.; Carretero, C.; Acero, J.; Alonso, R.; Burdio, J.M. Frequency-Dependent Resistance of Planar Coils in Printed Circuit Board With Litz Structure. *IEEE Trans. Magn.* **2014**, *50*, 8402409. [CrossRef]